

## RESEARCH ARTICLE

## Single-photon-level light storage with distributed Rydberg excitations in cold atoms

Hanxiao Zhang<sup>1</sup>, Jinhui Wu<sup>1,†</sup>, M. Artoni<sup>2</sup>, G. C. La Rocca<sup>3</sup><sup>1</sup>Center for Quantum Sciences and School of Physics, Northeast Normal University, Changchun 130024, China<sup>2</sup>Department of Engineering and Information Technology and Istituto Nazionale di Ottica (INO-CNR),  
Brescia University, 25133 Brescia, Italy<sup>3</sup>Scuola Normale Superiore and CNISM, 56126 Pisa, ItalyCorresponding author. E-mail: [†jhwu@nenu.edu.cn](mailto:†jhwu@nenu.edu.cn)

Received May 12, 2021; accepted July 14, 2021

We present an improved version of the superatom (SA) model to examine the slow-light dynamics of a few-photons signal field in cold Rydberg atoms with van der Waals (vdW) interactions. A main feature of this version is that it promises consistent estimations on total Rydberg excitations based on dynamic equations of SAs or atoms. We consider two specific cases in which the incident signal field contains more photons with a smaller detuning or less photons with a larger detuning so as to realize the single-photon-level light storage. It is found that vdW interactions play a significant role even for the slow-light dynamics of a single-photon signal field as distributed Rydberg excitations are inevitable in the picture of dark-state polariton. Moreover, the stored (retrieved) signal field exhibits a clearly asymmetric (more symmetric) profile because its leading and trailing edges undergo different (identical) traveling journeys, and higher storage/retrieval efficiencies with well preserved profiles apply only to weaker and well detuned signal fields. These findings are crucial to understand the nontrivial interplay of single-photon-level light storage and distributed Rydberg excitations.

**Keywords** few-photons light storage, distributed Rydberg excitation, cold Rydberg atom, improved superatom model

## 1 Introduction

In the 20th century, people have been guided by extensive studies in optics and photonics into the intriguing world of quantum physics and quantum information. Photon-based schemes exhibiting obvious advantages like fast and parallel operations have flourished in both quantum communication and quantum computation tasks, including long-range secure quantum cryptography [1, 2], quantum repeater [3], and quantum information encoding [4]. It is still a great challenge, however, to achieve effective interactions between individual photons, though various schemes have been proposed to generate strongly interacting photons based, e.g., on cavity quantum electrodynamics systems assisted with atoms [5–7].

Interactions of photons may also be achieved through electromagnetically induced transparency (EIT), a well-known quantum interference effect that can largely modify near-resonant optical properties of coherently driven atomic media and metamaterials [8–10]. For instance,

EIT can significantly enhance the Kerr nonlinearity and well suppress the linear absorption, both needed to achieve effective photonic phase gates [11–13]. Rydberg atoms, on the other hand, have been widely exploited to seek alternative quantum manipulation schemes, not only because they exhibit long radiative lifetimes and strong dipole-dipole interactions [14], but also because they are easy to combine with the EIT techniques [15–17]. Within this context, Rydberg-EIT media have been used to achieve single photon manipulation [18–21], cooperative optical nonlinearity [22], and photons bound states [23–25].

Neighboring Rydberg atoms exhibit, in turn, strong van der Waals (vdW) interactions that may lead to dipole blockade [26–29], known to prohibit the simultaneous excitations of two (or more) atoms to the same and different Rydberg states. A superatom (SA) model [30, 31] in the mean-field sense is commonly adopted to treat the nonlinear spectra based on dipole blockade in Rydberg-EIT media. This effective model has been extended [32] to partially recover experiments on slow-light propagation in cold Rydberg atoms [33–39], where intriguing effects such as sub-Poissonian statistics, storage enhanced interactions, and microwave induced exchanges of Rydberg dark-state polaritons are recently observed. On a differ-

\* This article can also be found at <http://journal.hep.com.cn/fop/EN/10.1007/s11467-021-1105-6>.



ent tack and unrelated to the SA model, efforts have also been made [40–43] to devise theoretical schemes that deal with slow-light propagation and interaction in Rydberg-EIT media. These are schemes based, e.g., on open spin or effective field theories that use different degrees of approximation to relax the complexity of many-body photon(s) propagation problems in actual experiments.

In this paper we address the nontrivial interplay between spatially distributed Rydberg excitations and nonlinear light storage in a Rydberg-EIT medium, based on an improved SA model enabling deeper insights into the slow-light dynamics of a few-photons signal. This model provides consistent estimates on the total Rydberg excitations during light storage via two independent integration procedures, while ensuring an effective coupling to Rydberg atoms even if the signal is in the single-photon state. Our findings are supported by numerical calculations carried out for both an incident well detuned weaker signal and an incident nearly resonant stronger signal. We confirm, in particular, that vdW interactions ought to be taken into account even for a single-photon signal pulse as its slow-light dynamics must result in a dark-state polariton [43] with distributed Rydberg excitations. We also observe that the stored (retrieved) signal has a clearly asymmetric (more symmetric) profile as its leading and trailing edges suffer fairly different (roughly identical) nonlinear absorption and dispersion while propagating through the Rydberg-EIT medium. Last but not least, it is found that weaker and well detuned incident signals are largely insensitive to the nonlinear absorption and dispersion arising from distributed Rydberg excitations and hence are beneficial to improve the storage/retrieval efficiency and preserve the space-time profile.

## 2 Model and methods

Here we examine the storage and retrieval dynamics of a *quantum signal pulse* of electric field (frequency)  $\hat{\mathcal{E}}_s$  ( $\omega_s$ ) traveling along the  $z$  axis in a cold sample of stationary atoms illuminated by a *classical control beam* of amplitude (frequency)  $E_c$  ( $\omega_c$ ) [see Fig. 1(a)]. Relevant Rabi frequencies and detunings are defined, respectively, as  $\Omega_s = \kappa \mathcal{E}_s$ ,  $\Omega_c = E_c d_{er} / (2\hbar)$  and  $\delta = \omega_s - \omega_{ge}$ ,  $\Delta = \omega_s + \omega_c - \omega_{gr}$  [see Fig. 1(b)]. Here  $d_{ij}$  ( $\omega_{ij}$ ) denotes the dipole moment (resonant frequency) on transition  $|i\rangle \leftrightarrow |j\rangle$  while  $\kappa = d_{ge} \sqrt{\omega_s} / (2\hbar \epsilon_0 V)$  represents the coupling constant for signal photons of quantum volume  $V$ . The atoms exhibit a three-level ladder configuration involving the ground state  $|g\rangle$ , the intermediate state  $|e\rangle$ , and the Rydberg state  $|r\rangle$ , a pair of which located respectively at  $z$  and  $z'$  will interact through the vdW potential  $\mathcal{V}(z - z') = C_6 / |z - z'|^6$  when both excited to the Rydberg state. The vdW coefficient takes the value  $C_6 = 6.5 \times 2\pi \times 10^{12} \text{ s}^{-1} \mu\text{m}^6$  in the case of  $|g\rangle \equiv |5S_{1/2}, F = 2, m_F = 2\rangle$ ,  $|e\rangle \equiv |5P_{3/2}, F = 3, m_F = 3\rangle$ ,

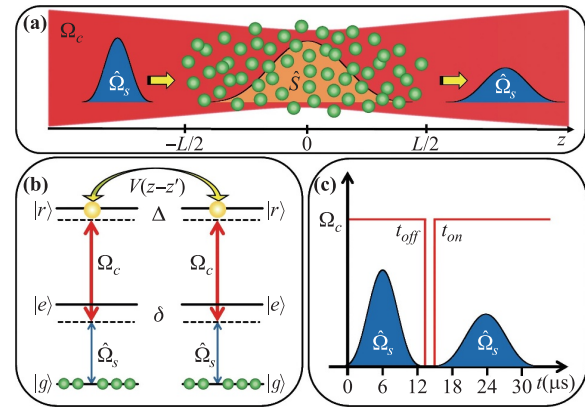


**Fig. 1** (a) Schematic illustration of a storage and retrieval process where the *slow-light* signal field  $\hat{\mathcal{E}}_s$  ( $\Omega_s$ ) is mapped into and then recovered from the *stationary* spin field  $\hat{S}$  in a sample of cold atoms with switching off and then back on the control field  $E_c$  ( $\Omega_c$ ). (b) A ladder level configuration driven by the signal field of Rabi frequency (detuning)  $\Omega_s$  ( $\delta$ ) on transition  $|g\rangle \leftrightarrow |e\rangle$  and the control field of Rabi frequency (detuning)  $\Omega_c$  ( $\Delta - \delta$ ) on transition  $|e\rangle \leftrightarrow |r\rangle$ . Two atoms also exhibit the separation-dependent vdW potential  $\mathcal{V}(z - z')$  when both are in Rydberg state  $|r\rangle$ . (c) A time sequence for the storage and retrieval process, in which field  $\hat{\Omega}_s$  is incident at  $t = 0$  while field  $\Omega_c$  is switched off (on) at  $t_{off}$  ( $t_{on}$ ).

and  $|r\rangle \equiv |83S_{1/2}, m_J = 1/2\rangle$  for the  $^{87}\text{Rb}$  atoms [44]. A typical three-stage (time) excitation sequence for a signal taken in the form of a Gaussian pulse (see Section 3) is illustrated in Fig. 1(c). We further introduce the polarization  $\hat{P} = \sqrt{N} \hat{\sigma}_{ge}$  and the spin field  $\hat{S} = \sqrt{N} \hat{\sigma}_{gr}$  in terms of the atomic transition operators  $\hat{\sigma}_{ge} = |g\rangle \langle e|$  and  $\hat{\sigma}_{gr} = |g\rangle \langle r|$  [45], with  $N$  denoting the homogeneous atomic density. In the limit of low atomic excitations ( $\sigma_{ge} \rightarrow 0$  and  $\sigma_{gr} \rightarrow 0$ ) [46], these operators satisfy the same-time commutation relations  $[\hat{\mathcal{E}}_s(z, t), \hat{\mathcal{E}}_s^\dagger(z', t)]/V = [\hat{P}(z, t), \hat{P}^\dagger(z', t)] = [\hat{S}(z, t), \hat{S}^\dagger(z', t)] = \delta(z - z')$ .

Then we can write down the Hamiltonians [47]

$$\begin{aligned} \hat{H}_{tot} &= \hat{H}_{ph} + \hat{H}_{cp} + \hat{H}_{int}, \\ \hat{H}_{ph} &= -i\hbar c \int_0^L dz \hat{\mathcal{E}}_s^\dagger(z, t) \partial_z \hat{\mathcal{E}}_s(z, t), \\ \hat{H}_{cp} &= -\hbar \int_0^L dz [\sqrt{N} \hat{\Omega}_s^\dagger(z, t) \hat{P}(z, t) + h.c.] \\ &\quad - \hbar \int_0^L dz [\Omega_c(t) \hat{S}^\dagger(z, t) \hat{P}(z, t) + h.c.] \\ &\quad - \hbar \int_0^L dz [\delta \hat{P}^\dagger(z, t) \hat{P}(z, t) + \Delta \hat{S}^\dagger(z, t) \hat{S}(z, t)], \\ \hat{H}_{int} &= \frac{\hbar}{2} \int_0^L \int_0^L dz dz' [\hat{S}^\dagger(z, t) \hat{S}^\dagger(z', t) \\ &\quad \mathcal{V}(z - z') \hat{S}(z', t) \hat{S}(z, t)], \end{aligned} \quad (1)$$

where the contributions  $\hat{H}_{ph}$ ,  $\hat{H}_{cp}$ , and  $\hat{H}_{int}$  have the usual interpretations [47] with respect to the kinetic energy,

atom-photon couplings, and dipole-dipole interactions, respectively. The corresponding Heisenberg equations can be obtained from  $\hat{H}_{tot}$  and read as

$$\begin{aligned}\partial_t \hat{P} &= -(\gamma_e - i\delta)\hat{P} + i\Omega_c^* \hat{S} + i\sqrt{N}\hat{\Omega}_s, \\ \partial_t \hat{S} &= -[\gamma_r - i(\Delta - \Delta_v)]\hat{S} + i\Omega_c \hat{P}, \\ \partial_t \hat{\Omega}_s &= -c\partial_z \hat{\Omega}_s + i\kappa^2 V \sqrt{N} \hat{P},\end{aligned}\quad (2)$$

where  $\gamma_e$  ( $\gamma_r$ ) is the dephasing rate on transition  $|g\rangle \leftrightarrow |e\rangle$  ( $|e\rangle \leftrightarrow |r\rangle$ ). It is worth noting that the nonlocal term  $\Delta_v$  denotes the expectation value

$$\Delta_v(z) = \frac{1}{2} \int_0^L dz' [\hat{S}^\dagger(z', t) \mathcal{V}(z - z') \hat{S}(z', t)],$$

which refers to the vdW induced shift of state  $|r\rangle$ . This fully describes the slow-light dynamics of signal ( $\hat{\Omega}_s$ ) yet makes Eq. (2) difficult to solve.

In the spirit of a mean-field sense, we now develop an improved version of the SA model [30] to solve Eq. (2) by providing an estimate of the total Rydberg excitations that is consistent with dynamic equations for SAs as well as with dynamic equations for atoms. Each SA is defined here as an ensemble of  $n_b = NV_b$  atoms in the thin and short cylinder of volume  $V_b = 2\pi R_b R_s^2$  with half blockade length  $R_b = [C_6(\delta^2 + \gamma_e^2)/(\delta + \gamma_e)|\Omega_c|^2]^{1/6}$  [48] and signal beam radius  $R_s \leq R_b$ . The SAs should be described by  $3^{n_b}$  collective states among which  $|G\rangle$  is the ground state while  $|E^{(1)}\rangle$  and  $|R^{(1)}\rangle$  are the first-order states [31]. Higher-order SA states involving two or more excitations in atomic state  $|r\rangle$  ( $|e\rangle$ ) can be safely ignored because they are strictly forbidden (greatly suppressed) owing to the dipole blockade (EIT) effect [31] in the parameter regime of our interest. Then we can define  $\hat{\Sigma}_{IJ} = |I\rangle\langle J|$  as the SA transition ( $I \neq J$ ) or projection ( $I = J$ ) operators with  $\{I, J\} \in \{G, E^{(1)}, R^{(1)}\}$ .

For the  $n_b$  atoms in a given SA, their (average) vdW induced shift can be expressed as  $\Delta_v = \bar{\Delta}\Sigma_{RR} + \bar{\delta}\bar{\Sigma}_{RR}$ , being  $\bar{\Delta} \rightarrow \infty$  weighted by the local Rydberg population  $\Sigma_{RR}$  inside of this SA while  $\bar{\delta} = \Omega_c^2/(8\gamma_e)$  weighted by the average Rydberg population  $\bar{\Sigma}_{RR}$  outside of this SA [30, 31]. As shown in the next section, both  $\Sigma_{RR}$  and  $\bar{\Sigma}_{RR}$  are very small and of the same order, so it is appropriate to take  $\Delta_v = \bar{\Delta}\Sigma_{RR}$  in the following. Accordingly, we have a two-level absorbing system for the  $\Sigma_{RR}$  fraction of SAs after taking  $\bar{\Delta} \rightarrow \infty$  into Eq. (2), while a three-level EIT system for the  $1 - \Sigma_{RR}$  fraction of SAs after taking  $\bar{\Delta} \rightarrow 0$  into Eq. (2) [49]. Then, replacing operators  $\hat{O}$  with their expectation values  $O$ , we can recast Eq. (2) into the following set of coupled equations

$$\begin{aligned}\partial_t \Sigma_{GG} &= 2\gamma_e \Sigma_{EE} - i\sqrt{n_b}\Omega_s \Sigma_{EG} + i\sqrt{n_b}\Omega_s^* \Sigma_{GE}, \\ \partial_t \Sigma_{EE} &= -2\gamma_e \Sigma_{EE} + 2\gamma_r \Sigma_{RR} - i\Omega_c \Sigma_{RE} + i\Omega_c^* \Sigma_{ER} \\ &\quad + i\sqrt{n_b}\Omega_s \Sigma_{EG} - i\sqrt{n_b}\Omega_s^* \Sigma_{GE}, \\ \partial_t \Sigma_{GE} &= -(\gamma_e - i\delta)\Sigma_{GE} + i\Omega_c^* \Sigma_{GR} \\ &\quad - i\sqrt{n_b}\Omega_s (\Sigma_{EE} - \Sigma_{GG}),\end{aligned}\quad (3)$$

$$\begin{aligned}\partial_t \Sigma_{GR} &= -(\gamma_r - i\Delta)\Sigma_{GR} + i\Omega_c \Sigma_{GE} - i\sqrt{n_b}\Omega_s \Sigma_{ER}, \\ \partial_t \Sigma_{ER} &= -(\gamma_e + \gamma_r - i\Delta + i\delta)\Sigma_{ER} \\ &\quad - i\Omega_c (\Sigma_{RR} - \Sigma_{EE}) - i\sqrt{n_b}\Omega_s^* \Sigma_{GR},\end{aligned}$$

for the three-level SA;

$$\partial_t P_2 = -(\gamma_e - i\delta)P_2 + i\sqrt{N}\Omega_s, \quad (4)$$

for the two-level atom;

$$\begin{aligned}\partial_t P_3 &= -(\gamma_e - i\delta)P_3 + i\Omega_c^* S + i\sqrt{N}\Omega_s, \\ \partial_t S &= -(\gamma_r - i\Delta)S + i\Omega_c P_3,\end{aligned}\quad (5)$$

for the three-level atom;

$$c\partial_z \Omega_s = i\kappa^2 V \sqrt{N} [P_2 \Sigma_{RR} + P_3 (1 - \Sigma_{RR})], \quad (6)$$

for the signal field. These equations are attained indeed with the following few considerations. First, we work in a regime where the SA population  $\Sigma_{RR}$  is much larger than its atomic counterpart  $\sigma_{rr}$  and non negligible even for very weak signals [50]; all elements  $\Sigma_{IJ}$  have then been included in Eq. (3) with the constraints  $\Sigma_{IJ} = \Sigma_{JI}^*$  and  $\Sigma_{GG} + \Sigma_{EE} + \Sigma_{RR} = 1$ . Second, we remove the term  $\partial_t \Omega_s$  from the left side of Eq. (6) as appropriate to the slow-light regime of our interest. Finally, we recall that the two-particle (vdW) interactions will modify the signal's photon statistics, which can be quantified by introducing the two-photon correlation function [31, 51]

$$g_s(z, t) = \frac{\langle \hat{\mathcal{E}}_s^\dagger(z, t) \hat{\mathcal{E}}_s^\dagger(z, t) \hat{\mathcal{E}}_s(z, t) \hat{\mathcal{E}}_s(z, t) \rangle}{\langle \hat{\mathcal{E}}_s^\dagger(z, t) \hat{\mathcal{E}}_s(z, t) \rangle \langle \hat{\mathcal{E}}_s^\dagger(z, t) \hat{\mathcal{E}}_s(z, t) \rangle}$$

as further discussed below. It is worth noting that  $g_s$  does not appear to modify  $\Sigma_{IJ}$  and thus  $\Omega_s$  as it is absent in the dynamic equations of both SAs and atoms. Including  $g_s$  in the dynamic equations of only SAs would lead to inconsistent estimates on the total Rydberg excitations obtained with  $\Sigma_{RR}$  and  $|S|^2$ , respectively. Including  $g_s$  in the dynamic equations of both SAs and atoms, though generating consistent estimates on the total Rydberg excitations, is also incorrect because a signal field in the single-photon Fock state ( $g_s = 0$ ) becomes decoupled from the Rydberg-EIT medium. Within the present slow-light regime,  $g_s$  can be computed with

$$c\partial_z g_s = -\kappa^2 V \sqrt{N} \text{Im}[\Sigma_{RR}(P_2 - P_3)/\Omega_s] g_s, \quad (7)$$

to account for two-particle (vdW) interactions.

With the help of Eqs. (3)–(6) we can now compute the number of *incident* signal photons  $N_s^{in} \equiv N_s(z = 0)$  and that of *retrieved* signal photons  $N_s^{re} \equiv N_s(z = L)$  outside the Rydberg-EIT medium

$$N_s(z) = \frac{\hbar\epsilon_0 \lambda_s R_s^2}{d_{ge}^2} \int_{-\infty}^{\infty} |\Omega_s(z, t)|^2 dt, \quad (8)$$

with the consideration of  $N_s(z)\hbar\omega_s = \pi R_s^2 \int_0^\infty I_s(z, t) dt$  as well as  $I_s(z, t) = 2\hbar^2 c \epsilon_0 |\Omega_s(z, t)|^2 / d_{ge}^2$ . The number

of stored signal photons inside the Rydberg-EIT medium, however, should be computed with

$$N_s^{st} = \frac{\hbar\epsilon_0\lambda_s R_s^2}{d_{ge}^2 v_g} \int_0^L |\Omega_s(z, t_1)|^2 dz, \quad (9)$$

being  $v_g$  the group velocity of a slowly propagating signal and  $t_1$  (slightly smaller than  $t_{off}$ ) the time when the control field starts to decrease. The number of distributed Rydberg excitations, in particular, will be estimated in two consistent ways. The *first* is

$$n_{ryd}^{at} = \pi R_s^2 \int_0^L [1 - \Sigma_{RR}(z, t_2)] |S(z, t_2)|^2 dz, \quad (10)$$

which denotes the total Rydberg excitations contributed by the  $(1 - \Sigma_{RR})$  fraction of atoms, *i.e.*, those described by the three-level EIT configuration, since  $\pi R_s^2 |S|^2 dz = N |\sigma_{rr}| dV$ . It is then appropriate to further introduce the effective spin field  $S' = S\sqrt{1 - \Sigma_{RR}}$  by excluding all two-level absorbing atoms. The *second* is

$$n_{ryd}^{sa} = \frac{1}{2R_b} \int_0^L \Sigma_{RR}(z, t_2) dz, \quad (11)$$

which denotes the total Rydberg excitations contributed by all  $L/2R_b$  SAs with  $\int_0^L (\Sigma_{RR}/L) dz$  being the average population. Here  $t_2$  (slightly larger than  $t_{off}$ ) is the time when the control field just decreases to zero.

The steady state solutions of Eq. (5) and Eq. (6)

$$P_2 = \sqrt{N} \sigma_{ge}^{(2)} = \frac{i\sqrt{N}\Omega_s}{\gamma_e - i\delta}, \quad (12a)$$

$$P_3 = \sqrt{N} \sigma_{ge}^{(3)} = \frac{i(\gamma_r - i\Delta)\sqrt{N}\Omega_s}{(\gamma_e - i\delta)(\gamma_r - i\Delta) + |\Omega_c|^2}, \quad (12b)$$

$$S = \sqrt{N} \sigma_{gr}^{(3)} = \frac{-\sqrt{N}\Omega_s\Omega_c}{(\gamma_e - i\delta)(\gamma_r - i\Delta) + |\Omega_c|^2}. \quad (12c)$$

enable one to attain the atomic population

$$\sigma_{rr} \equiv \sigma_{rg}^{(3)} \sigma_{gr}^{(3)} = \frac{|\Omega_s|^2 |\Omega_c|^2}{\gamma_e^2 \Delta^2 + (|\Omega_c|^2 - \delta \Delta)^2}, \quad (13)$$

whose maxima and half maxima are at

$$\Delta_{max} = \delta \times \frac{|\Omega_c|^2}{\delta^2 + \gamma_e^2}; \quad \Delta_{half}^{\pm} = (\delta \pm \gamma_e) \times \frac{|\Omega_c|^2}{\delta^2 + \gamma_e^2}$$

in the limit of  $\gamma_r \rightarrow 0$  for a fixed  $\delta$ . In fact, we have used  $\Delta_{half}^+$  to define the blockade radius  $R_b$  because  $C_6$  is positive. With  $\chi_s^{(3)} = (1 - \Sigma_{RR})N|d_{ge}|^2\sigma_{ge}^{(3)}/(\hbar\epsilon_0\Omega_s)$ , we can also attain the group velocity at  $\Delta = 0$

$$v_g = \frac{\lambda_s}{\pi\partial\chi_s^{(3)}/\partial\Delta} = \frac{\hbar\epsilon_0\lambda_s|\Omega_c|^2}{\pi N|d_{ge}|^2(1 - \Sigma_{RR})}, \quad (14)$$

which will change more or less during the slow-light signal propagation depending on the local value of  $\Sigma_{RR}$ . We

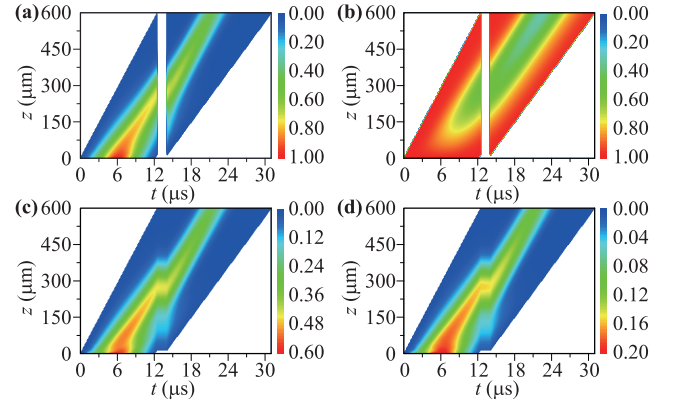


**Fig. 2** Space-time evolutions of the scaled pulse intensity  $|\Omega_s/\Omega_s^m|^2$  (a), the two-photon correlation  $g_s$  (b), the scaled magnitude square of spin field  $10^5|S'|^2/N$  (c), and the SA Rydberg population  $\Sigma_{RR}$  (d) in case (i). The control and signal fields have parameters  $\Delta = 0$ ,  $\Omega_c = 2\pi \times 2.3$  MHz,  $\delta = 2\pi \times 18$  MHz,  $\Omega_s^m = 2\pi \times 6.0$  kHz,  $t_s = 6.0$   $\mu\text{s}$ ,  $\delta t_s = 5.0$   $\mu\text{s}$ ,  $t_{off} = 12.5$   $\mu\text{s}$ ,  $t_{on} = 14.0$   $\mu\text{s}$ ,  $\lambda_s = 780$  nm, and  $R_s = 14.0$   $\mu\text{m}$ . The Rydberg-EIT medium has parameters  $\gamma_e = 2\pi \times 6.0$  MHz,  $\gamma_r = 2\pi \times 2.0$  kHz,  $d_{ge} = 2.534 \times 10^{-29}$  C·m,  $N_0 = 1.8 \times 10^{12}$   $\text{cm}^{-3}$ ,  $L = 600$   $\mu\text{m}$ , and  $R_b = 16.4$   $\mu\text{m}$ .

finally find  $N_s^{st} = n_{ryd}^{at}$  and  $n_{ryd}^{at} = n_{ryd}^{sa}$  at  $\Delta = 0$  by taking  $\Sigma_{RR} = n_b|\Omega_s|^2/(n_b|\Omega_s|^2 + |\Omega_c|^2)$  [30] and  $n_b = 2\pi NR_b R_s^2$  as well as  $v_g$  in Eq. (14) and  $S$  in Eq. (12c) back to Eqs. (9)–(11). The former equality  $N_s^{st} = n_{ryd}^{at}$  suggests that a Rydberg dark-state polariton [43] is formed as the number of stored signal photons is identical to the number of total Rydberg excitations. The latter equality  $n_{ryd}^{at} = n_{ryd}^{sa}$  [52] is naturally required in a valid SA model as both  $n_{ryd}^{at}$  and  $n_{ryd}^{sa}$  refer to the number of total Rydberg excitations, though attained from dynamic equations of atoms and those of SAs, respectively.

### 3 Results and discussion

In this section, we present numerical simulations on the nontrivial slow-light propagation in a cold Rydberg-EIT medium under two-photon resonance ( $\Delta = 0$ ) using the improved SA model. In particular, we aim at examining whether storing the same number of signal photons can be realized with different combinations of  $\delta$  and  $\Omega_s^m$  and in the presence of different dynamic behaviors. The simulations proceed from an incident (Gaussian) signal with field amplitude  $\Omega_s(0, t) = \Omega_s^m e^{-(t-t_s)^2/\delta t_s^2}$  and two-photon correlation  $g_s(0, t) = 1$ , as appropriate for an ideal (coherent state) laser. These numerical results enable us to ascertain two representative cases of the pulse dynamics: (i) the incident signal is a well detuned weaker pulse with  $\Omega_s^m/(2\pi) = 6$  kHz ( $N_s^{in} \simeq 2.0$ ) and  $\delta/(2\pi) = 18$  MHz, and (ii) the incident signal is a nearly resonant stronger pulse with  $\Omega_s^m/(2\pi) = 16$  kHz ( $N_s^{in} \simeq 14.0$ ) and  $\delta/(2\pi) = 8$  MHz. The two cases confirm that storing the  $N_s^{st} \simeq 1.0$